Near-infrared autofluorescence imaging of cutaneous melanins and human skin *in vivo*

Xiao Han*
Harvey Lui
David I. McLean
Haishan Zeng
Laboratory for Advanced Medical Photonics (LAMP)
Cancer Imaging Department
British Columbia Cancer Research Centre
    and
Photomedicine Institute
Department of Dermatology and Skin Science
University of British Columbia and Vancouver Coastal
    Health Research Institute
Vancouver, British Columbia V5Z 1L3
Canada

Abstract. In recent years, near-infrared (NIR) autofluorescence imaging has been explored as a novel technique for tissue evaluation and diagnosis. We present an NIR fluorescence imaging system optimized for the dermatologic clinical setting, with particular utility for the direct characterization of cutaneous melanins *in vivo*. A 785-nm diode laser is coupled into a ring light guide to uniformly illuminate the skin. A bandpass filter is used to purify the laser light for fluorescence excitation, while a long-pass filter is used to block the main laser wavelength but pass the spontaneous components for NIR reflectance imaging. A computer-controlled filter holder is used to switch these two filters to select between reflectance and fluorescence imaging modes. Both the reflectance and fluorescence photons are collected by an NIR-sensitive charge-coupled device (CCD) camera to form the respective images. Preliminary results show that cutaneous melanin in pigmented skin disorders emits higher NIR autofluorescence than surrounding normal tissue. This confirmed our previous findings from NIR fluorescence spectroscopy study of cutaneous melanins and provides a new approach to directly image the distributions of cutaneous melanins in the skin. *In-vivo* NIR autofluorescence images may be useful for clinical evaluation and diagnosis of pigmented skin lesions, including melanoma. © *2009 Society of Photo-Optical Instrumentation Engineers.* [DOI: 10.1117/1.3103310]

1 Introduction

NIR fluorescence imaging can be a potentially useful technology for clinical dermatologic diagnosis due to the deeper penetration and minimal biological effects on skin of NIR radiation versus ultraviolet (UV) and short wavelength visible light. Although some *in-vitro* studies have been done for tissue samples with NIR autofluorescence,[1–4] not much progress has been made on *in-vivo* studies prior to our work,[5–7] especially for human subjects in clinical settings. One reason is that native tissue molecules usually emit very weak fluorescence under NIR light excitation.[8] Although exogenous fluorophores can be applied to enhance signal levels, this adds complications to the imaging process, not the least of which is the fact that such fluorophores must be considered as drugs in the clinical and regulatory context. Another reason is the difficulty of eliminating background fluorescence in the NIR range, which comes from various optical components within the imaging system. Those two factors in combination may

yield poor *in-vivo* NIR fluorescence images due to low signal-to-background ratio (SBR).

Important tissue fluorophores, such as elastin, collagen, and NADH, mostly fluoresce only under UV or short wavelength visible light excitation, and will appear dark under NIR excitation. Recently, a spectroscopic study of skin by our group[6] and an ophthalmologic imaging study by Keilhauer and Delori[9] have surprisingly found that melanin in human and animal tissue emits strong fluorescence under NIR excitation. This finding provides a rationale for practical *in-vivo* NIR fluorescence imaging of human tissue based on melanin as an endogenous fluorophore. In dermatology, melanin is a major tissue chromophore that plays a role in many benign and malignant skin disorders, including melanoma. Under UV and shorter wavelength visible light excitation, melanin has been found to have a much lower fluorescence signal than other tissue components.[10–15] Prior to our observation, the conventional approach to identifying cutaneous melanin essentially relied on measuring the amount of UV and shorter wavelength visible light that has been absorbed. To quantify the concentration of melanin in human skin, empirically based algorithms were developed to extract melanin's information

*Currently with the Department of Radiology, The University of Chicago.
Address all correspondence to: Dr. Haishan Zeng, Cancer Imaging Department, British Columbia Cancer Research Centre, 675 West 10th Avenue, Vancouver, BC, Canada V5Z 1L3. Tel: 604–675–8083; Fax: 604–675–8099; E-mail: hzeng@bccrc.ca.
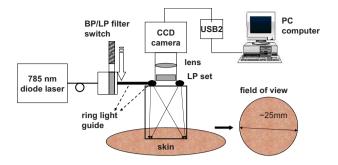
Fig. 1 Block diagram of the prototype NIR fluorescence imaging system.

from its reflectance spectra.[16] Nevertheless, it has not yet been possible to use a positive optical method to directly observe and potentially quantify cutaneous melanin. With NIR fluorescence, the optical signal that is directly emitted by melanin should provide more meaningful and complementary information on its distribution and biological activity within tissue.

Thus, based on our previous spectroscopic study,[6] and with special consideration given to optimizing an imaging system for NIR wavelengths, we have designed and constructed a prototype *in-vivo* NIR fluorescence imaging system for clinical skin evaluation. The specific goals of this work have been: 1. to visually confirm the melanin autofluorescence that was discovered through point spectroscopic measurements, and 2. to develop a clinically feasible method for exploiting this effect in the diagnosis and evaluation of pigmented skin disorders based on melanin NIR fluorescence imaging.

2 Materials and Methods

2.1 System Setup

Figure 1 shows the block diagram of the imaging system. Light from a solid-state diode laser (BRM-785-0.35-100-0.22-SMA B&W TEK Incorporated, Newark, Delaware; central wavelength: 785.113 nm, FWHM: 0.176 nm, power output: 350 mW) is coupled through a 200-μm optical fiber (P200-2-VIS/NIR, Ocean Optics Incorporated, Dunedin, Florida) to a ring light guide (Moritex USA Incorporated, San Jose, California; transmission $\approx$60% at 785 nm), which provides relatively uniform illumination at the end of the attached probe, with a field of view (FOV) of 25.0 mm in diameter. Reflectance and fluorescence photons remitted by the skin are then collected by a lens (Xenoplan 1.4/17 mm, Schneider Optics Incorporated, Hauppauge, New York), optimized for the wavelength range of 400 to 1000 nm, toward an NIR-sensitive camera (Alta U1, Apogee Instruments Incorporated, Roseville, California) for image acquisition. The camera incorporates a Kodak 0402-ME charge-coupled device (CCD) sensor with 9-μm square pixels in a 768×512 array, and operates at -20.0 ± 0.1 °C by a software-controlled on-board thermoelectric cooler and fan system. Data acquired by the camera are transferred to a PC system via a USB2 cable (480 MB/s data rate).

The system is designed to perform both NIR reflectance and fluorescence imaging within a clinically practical measurement time (in the order of a few seconds) with fast switching between the two imaging modes by placing appropriate optical filters at the illumination side (i.e., between the laser output and the ring light guide) and the light collection side (i.e., between the ring light guide and the lens) of the system. For reflectance imaging mode, a colored glass long-pass (LP) filter (RG-830, Edmund Optics Incorporated, Barrington, New Jersey) is used to select the NIR spectral range for illumination, and, at the light collection side, an LP filter combination consisting of two colored glass LP filters (RG-830, Edmund Optics Incorporated, Barrington, New Jersey) and an interference filter (RazorEdge Long Wave Pass Edge Filter LP02-785RU-25, Semrock, Rochester, New York) is used to collect the diffusely reflected NIR photons. In such a configuration, the main peak of the laser output at 785 nm is blocked; the diffusely reflected photons in the broad, spontaneous emission tail (roughly 830 to 1000 nm) of the laser spectrum form the reflectance image.

To switch from NIR reflectance imaging mode to the NIR fluorescence imaging mode, a bandpass (BP) filter (Max-Line™ Laser-line Filter LL01-785-25, Semrock, Rochester, New York) is inserted (within ~0.2 sec) at the illumination side to replace the LP filter, which eliminates the spontaneous emission tail in the laser output, while the LP filters at the detection side are not changed. In the system, the filter switch is achieved by a computer-controlled actuator (PLB-50, Pacific Laser Equipment, Santa Ana, California), such that minimum perturbation to the system and the imaging procedure is involved. This design of using the same (laser) light source for both fluorescence excitation and reflectance imaging illumination made the system more compact and efficient in switching between the two imaging modes.

2.2 Clinical Measurements

The study was approved by the Clinical Research Ethics Board of the University of British Columbia (protocol C05-0569). Informed consent was obtained from every patient or volunteer who participated in the study. The illumination power density at the skin surface was measured to be 0.029 W/cm², an order of magnitude below the ANSI maximum permissible skin exposure limit of 0.296 W/cm² for a 785-nm cw laser beam.[17] The NIR autofluorescence images included in this study were acquired with an exposure time of 2 sec, while the NIR reflectance images were acquired within 1 sec. Before each measurement, the lesion and its surrounding skin were cleaned with an isopropyl alcohol wipe. The NIR fluorescence and reflectance images are taken sequentially by holding the camera probe in gentle and steady contact with the skin surface for a few seconds. A standard clinical color image is also acquired using a Nikon digital camera (model D100 with 60 mm Micro-Nikkor f/2.8 lens). The entire imaging procedure takes about 2 min. We are currently conducting a systematic clinical study using this prototype imaging system. Example images are discussed next.

3 Results and Discussion

Using the previous NIR autofluorescence imaging system, we have successfully acquired *in-vivo* images of various skin lesions. Figure 2 shows a benign junctional melanocytic nevus, a cherry angioma, and a superficial spreading melanoma. The left column shows standard color photographs of the three lesions. In the middle column are NIR reflectance images,
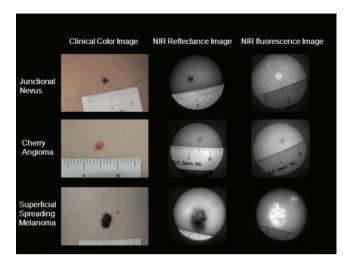
Fig. 2 Images from a benign junctional melanocytic nevus, a cherry angioma, and a superficial spreading melanoma. The left column is for clinical photographs, the middle column for NIR reflectance images, and the right column for NIR fluorescence images.
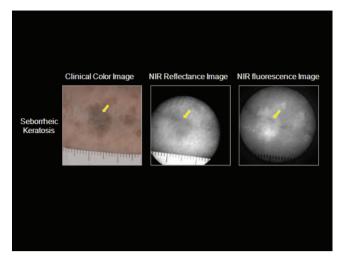

Fig. 3 Seborrheic keratosis overlapping a blood vessel: note that the yellow arrows point to where a blood vessel segment is relatively invisible in the clinical photographs and the NIR reflectance image. However, this blood segment is readily visible in the NIR fluorescence image.

while the right column shows the NIR fluorescence images. The junctional melanocytic nevus and the melanoma, both of which contain excessive melanin, showed significantly brighter NIR fluorescence emission than their surrounding normal skin, while their NIR reflectance images are darker than the surrounding normal skin due to melanin absorption of the incident light. Melanin absorption also accounts for their dark appearance in the color photographs. For comparison, images for a cherry angioma are shown in the second row; this type of skin lesion is a common benign neoplasm consisting of increased numbers of blood vessels in the skin. The lesion looks red on the clinical visible color image and dark on the NIR reflectance image due to hemoglobin absorption of the incident light from within the blood vessels of the lesion. In contrast, the NIR fluorescence image of a cherry angioma appears as a darker area compared to its surrounding normal skin. To quantitatively evaluate the results, we adopt the method used by Demos et al. in their study[3] and define the relative intensity difference $\Delta I\%$ as

$$\Delta I \% = \frac{|I_{\text{lesion}} - I_{\text{normal}}|}{I_{\text{normal}}},$$

where I_{lesion} is the image intensity averaged over the lesion and I_{normal} is the image intensity averaged over a normal region. For the junctional melanocytic nevus, I_{lesion} was estimated from a 144-pixel (~ 1 mm^2) area at the lesion, and I_{normal} was estimated from four such square areas in the surrounding normal region. The NIR reflectance image has $\Delta I\% = 0.53$ and the NIR autofluorescence image has $\Delta I\% = 0.66$. For the melanoma, I_{lesion} and I_{normal} are both estimated from four 144-pixel areas, sampled from the lesion and the surrounding normal region, respectively. The NIR reflectance image has $\Delta I\% = 0.46$ and the NIR autofluorescence image has $\Delta I\% = 0.65$.

These results confirm our previous point spectroscopy study results,[6] where cutaneous melanin fluoresces brightly under NIR excitation, and provide a new platform for imaging

the distributions of melanins in skin tissue *in vivo*. These results are also consistent with bright NIR fluorescence observed by Keilhauer et al.[9] for melanins in the ocular fundus.

Our study results provide a new method for imaging the distribution of skin melanins *in vivo*. While both reflectance imaging and NIR autofluorescence imaging are potentially useful for detecting melanins in tissue, the autofluorescence technique is perhaps especially favorable since it represents a "direct" method that also exhibits higher detection sensitivity. In other words, with the fluorescence method, an increase in signal is measured over a zero background signal, whereas with reflectance, the analogous signal (i.e., absorbed or scattered light) is derived "indirectly" as the difference between the incident and the reflected light. This small decrease in the intensity of a very large signal as measured in the reflectance technique leads to a correspondingly large loss in sensitivity.[18] Furthermore, for *in-vivo* skin tissue, the blood (hemoglobin) absorption is often of a comparable magnitude to melanin absorption, making it difficult to discern the true melanin distribution from single band reflectance imaging. Although there are more sophisticated ways, such as multispectral reflectance imaging, to differentiate these two chromophores, they require more complicated imaging hardware (in both optical components and imaging electronics), lengthened measurement time, complicated light transport modeling, and lengthy data processing time to derive the spatial distribution of these chromophores. In contrast, this issue is naturally solved by our system working in NIR autofluorescence mode, where melanin is a native fluorophore, while hemoglobin within blood vessels behaves as an absorbing chromophore. Figure 3 shows an incidental prominent blood vessel running beneath a melanin-rich seborrheic keratosis from upper left to middle right in the pictures. While the blood vessel is easily visible outside of the seborrheic keratosis on both the clinical visible color image and the NIR reflectance image, it is almost invisible within the lesion due to the confounding melanin absorption effect. On the other hand, the hemoglobin absorp-
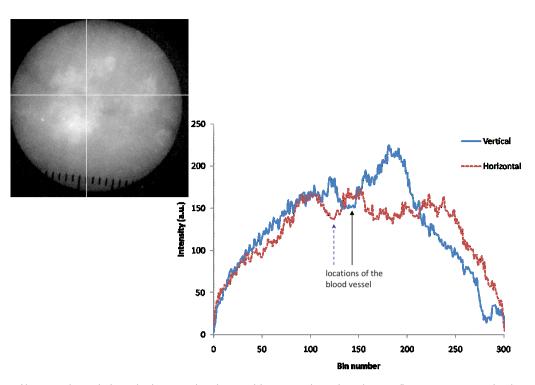
Fig. 4 Intensity profiles at each pixel along the horizontal and vertical lines as indicated on the NIR fluorescence image for the same seborrheic keratosis lesion shown in Fig. 3. When the lines are across the blood vessel locations, the image intensities are decreased.

tion also confounds the assessment of the melanin distribution from the reflectance images. Nevertheless, the NIR autofluorescence image in Fig. 3 clearly identified a segment of the blood vessel within the lesion as a dark spot (yellow arrow), while areas covered with melanins are bright. In Fig. 4, the profiles representing image intensities averaged from five adjacent vertical lines and five adjacent horizontal lines across the same lesion in Fig. 3 are plotted. Again, the NIR autofluorescence signal from the lesion clearly stands out above the normal skin background, while the blood vessel is recognized as decreased autofluorescence signals, as indicated by the arrows. This example demonstrated the great advantage of NIR autofluorescence imaging as a *direct* method for assessing cutaneous melanin distributions *in vivo* over the *indirect* reflectance imaging method.

4   Conclusions

We successfully develop a NIR fluorescence imaging system that can acquire good quality NIR autofluorescence images of the skin *in vivo* within a short, two-second exposure time that is suitable for clinical applications. The system can also acquire NIR reflectance images by utilizing spontaneous emission from the same laser within the same overall optical configuration. Preliminary results show that the distribution of NIR fluorescence due to cutaneous melanin within abnormally pigmented skin can be captured as an image showing a bright signal that corresponds directly to the presence of melanin. This has confirmed our previous findings from a NIR fluorescence point spectroscopy study of cutaneous melanins, and provides a new method for *directly* imaging the distributions of cutaneous melanins in skin tissue. The acquired

in-vivo NIR autofluorescence images may be useful for clinical evaluation and diagnosis of pigmented skin lesions, including melanoma. A systematic and detailed clinical study is underway in our laboratory to fully explore the clinical utility and limitations of this new imaging technique.

References

1. E. B. Hanlon, I. Itzkan, R. R. Dasari, M. S. Feld, R. J. Ferrante, A. C. McKee, D. Lathi, and N. W. Kowall, "Near-infrared fluorescence spectroscopy detects Alzheimer's disease in vitro," *Photochem. Photobiol.* **70**, 236–242 (1999).
2. G. Zhang, S. G. Demos, and R. R. Alfano, "Far-red and NIR Spectral wing emission from tissues under 532 and 632 nm photo-excitation," *Lasers Life Sci.* **9**, 1–16 (1999).
3. S. G. Demos, R. Gandour-Edwards, R. Ramsamooj, and R. White, "Near-infrared autofluorescence imaging for detection of cancer," *J. Biomed. Opt.* **9**(4), 587–592 (2004).
4. S. G. Demos, R. Gandour-Edwards, R. Ramsamooj, and R. White, "Spectroscopic detection of bladder cancer using near-infrared imaging techniques," *J. Biomed. Opt.* **9**(4), 767–771 (2004).
5. Z. Huang, H. Lui, D. I. McLean, M. Korbelik, and H. Zeng, "Raman spectroscopy in combination with background near-infrared autofluorescence enhances the in vivo assessment of malignant tissues," *Photochem. Photobiol.* **81**, 1219–1226 (2005).

6. Z. Huang, H. Zeng, I. Hamzavi, A. Alajlan, E. Tan, D. I. McLean, and H. Lui, "Cutaneous melanin exhibiting fluorescence emission under near-infrared light excitation," *J. Biomed. Opt.* **11**(3), 034010 (2006).

7. X. Han, H. Lui, D. I. McLean, and H. Zeng, "A technique for near-infrared autofluorescence imaging of skin: preliminary results," *Proc. SPIE* **6078**, 60780S (2006).

8. E. M. Sevick-Muraca, E. Kuwana, A. Godavarty, J. P. Houston, A. B. Thompson, and R. Roy, "Near-infrared fluorescence imaging and spectroscopy in random media and tissues," Chap. 33 in *Biomedical Photonics Handbook*, T. Vo-Dinh, Eds., pp. 33-1–33-66, CRC Press, Boca Raton, FL (2003).

9. C. N. Keilhauer and F. C. Delori, "Near-infrared autofluorescence imaging of the fundus: visualization of ocular melanin," *Invest. Ophthalmol. Visual Sci.* **47**, 3556–3564 (2006).

10. S. D. Kozikowski, L. J. Wolfram, and R. R. Alfano, "Fluorescence spectroscopy of eumelanins," *IEEE J. Quantum Electron.* **QE-20**, 1379–1382 (1984).

11. J. M. Gallas and M. Eisner, "Fluorescence of melanin-dependence upon excitation wavelength and concentration," *Photochem. Photobiol.* **45**, 595–600 (1987).

12. M. Elleder and J. Borovansky, "Autofluorescence of melanins induced by ultraviolet radiation and near ultraviolet light. A histochemical and biochemical study," *Histochem. J.* **33**, 273–281 (2001).

13. S. P. Nighswander-Rempel, J. Riesz, J. Gilmore, J. Bothma, and P. Meredith, "Quantitative fluorescence excitation spectra of synthetic eumelanin," *J. Phys. Chem. B* **109**, 20629–20635 (2005).

14. S. P. Nighswander-Rempel, J. Riesz, J. Gilmore, and P. Meredith, "A Quantum Yield Map for Synthetic Eumelanin," *J. Chem. Phys.* **123**, 194901 (2005).

15. P. Meredith, B. J. Powell, J. Riesz, S. P. Nighswander-Rempel, M. R. Pederson, and E. Moore, "Towards structure-property-function relationships for eumelanin," *Soft Matter* **2**, 37–44 (2006).

16. G. N. Stamatas, B. Z. Zmudzka, N. Kollias, and J. Z. Beer, "Noninvasive measurements of skin pigmentation *in situ*," *Pigment Cell Res.* **17**, 618–626 (2004).

17. *American National Standard for the Safe Use of Lasers*, ANSI Standard Z136.1-2007, American National Standards Institute, Washington, D.C. (2007).

18. H. Zeng, "Human skin optical properties and autofluorescence decay dynamics," PhD Thesis, pp. 109, University of British Columbia, Vancouver, BC (1993).